Supporting Information

Design and Synthesis of Non-Fullerene Acceptors Based on Quinoxalineimide Moiety as the Central Building Block for Organic Solar Cells

Chunguang Zhu, Kang An, Wenkai Zhong, Zhenye Li, Yu Qian, Xiaozhe Su, Lei Ying*

Institute of Polymer Optoelectronic Materials and Devices, State Key Laboratory of Luminescent Materials and Devices, South China University of Technology, Guangzhou, 510640, China

Email: msleiying@scut.edu.cn

Table of Contents

1. Material and Synthesis

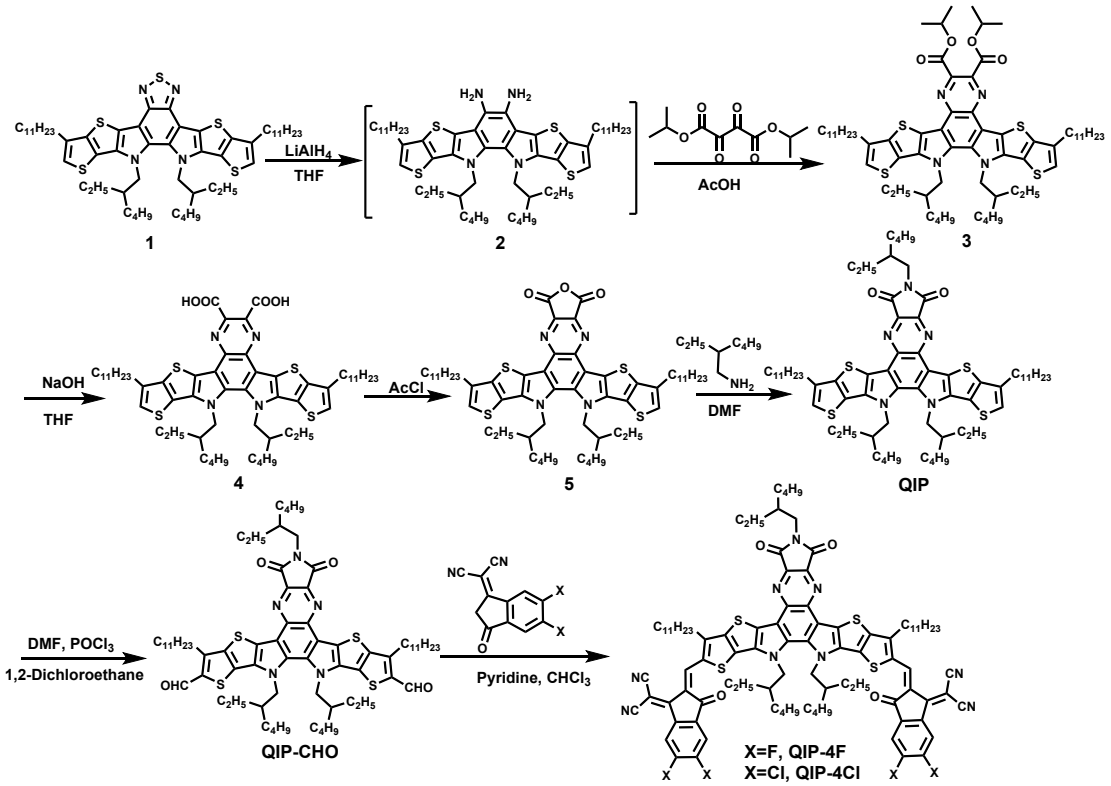

Scheme S1. Synthetic routes of QI-based FREAs (QIP-4F and QIP-4Cl).

Synthesis of QIP-4F and QIP-4Cl. All the chemical reagents were purchased from Chem Greatwall, Derthon, and Alfa Aesar, and used as received directly. 2-(5,6-difluoro-3-oxo-2,3-dihydro-1H-inden-1-ylidene)malononitrile and 2-(5,6-dichloro-3-oxo-2,3-dihydro-1H-inden-1-ylidene)malononitrile was purchased from Derthon OPV Co Ltd; 12,13-bis(2-ethylhexyl)-3,9-diundecyl-12,13-dihydro-[1,2,5]thiadiazolo[3,4-*e*]thieno[2

''',3'':4',5']thieno[2',3':4,5]pyrrolo[3,2-*g*]thieno[2',3':4,5]thieno[3,2-*b*]indole (1) and diisopropyl 2,3-dioxosuccinate were synthesized according to the reported literatures.[1-2]

Synthesis of compound 3.

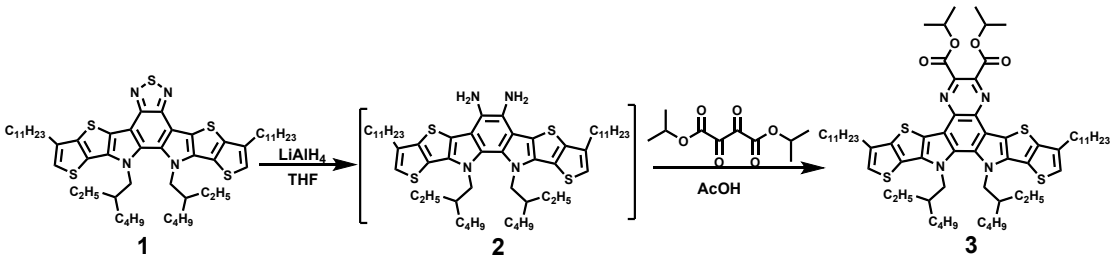

Under nitrogen, compound 1 (2.0 g, 2.06 mmol), $LiAlH_4$ (1.56 g, 41.17 mmol), and 30 mL of THF were added into a 100 mL flask. The mixed solution was stirred at 75 °C for 12 h. After cooling to room temperature, the mixture was extracted with dichloromethane, dried with anhydrous Na_2SO_4, filtered and concentrated under reduced pressure. A orange diamine 2 was obtained in high yields and used directly to synthesize the compound 3. Subsequently, a condensation coupling reaction between diamine 2 and diisopropyl 2,3-dioxosuccinate (1.46 g, 6.36 mmol) was performed at 80 °C in alcohol (30 mL). After 12 h, the organic phase was separated by extraction with dichlormethane and then dried over Na_2SO_4. Finally, dichlormethane was removed under reduced pressure to yield a red solid 3, which was further purified by column chromatography (petroleum ether/dichloromethane, v/v = 2:1) (1.62 g, 70 % for two steps). ^{1}H NMR (400 MHz, $CDCl_3$), δ (ppm): 7.03 (s, 2H), 5.50–5.44 (m, 2H), 4.70–4.61(m, 4H), 2.87–2.83 (t, 4H), 2.09–2.06 (t, 2H), 1.89–1.85 (t, 4H), 1.55–1.54 (d, 6H), 1.38–1.11(m, 36H), 1.10–0.86 (m, 24H), 0.64–0.60 (m, 12H); ^{13}C NMR (100 MHz, $CDCl_3$), δ (ppm): 165.32, 143.79, 140.86, 137.88, 136.97, 134.77, 131.73, 123.26, 122.44, 119.44, 117.37, 69.93, 55.00, 39.91, 31.92, 29.70, 29.67, 29.64, 29.63, 29.51, 29.50, 29.37, 28.84, 27.73, 27.70, 23.05, 22.99, 22.75, 22.70, 21.86, 14.12, 13.76,

10.05, 10.00. MALDI-TOF-MS: m/z = 1136.730 (M^+).

Synthesis of compound 4.

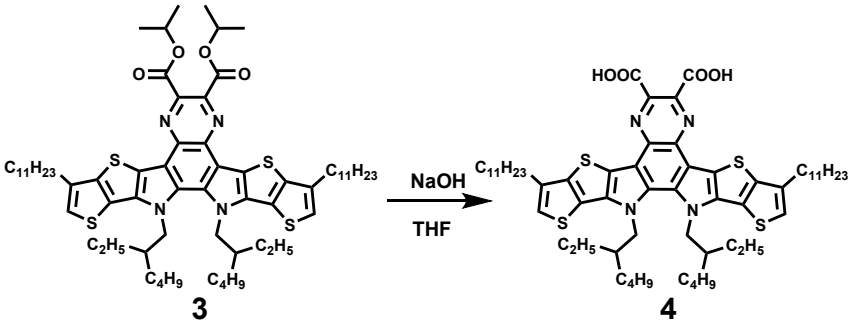

To a 200 mL three-neck round-bottomed flask, a mixture solution of compound 3 (1 g, 0.88 mmol), NaOH aq (3 M, 50 mL) and THF (50 mL) were added. Then the mixture was stirred at 60 °C for 12 hours. After the reaction, the reaction mixture was acidized with HCl aq to pH 1. Water was added, and the mixture was extracted with dichloromethane. The combined organic layer was dried over Na_2SO_4 and the solvent was removed under reduced pressure. The crude product was not purified and used directly for the next step. MALDI-TOF-MS: m/z = 1052.690 (M^+).

Synthesis of compound 5.

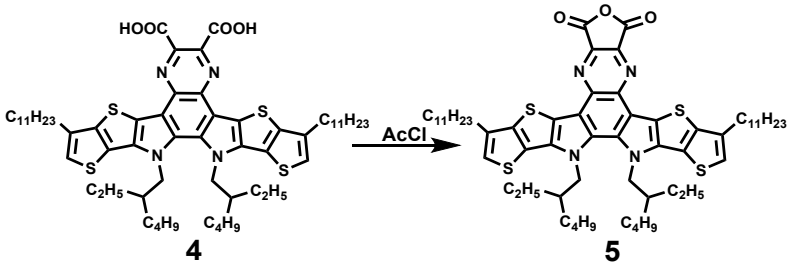

Under a N_2 atmosphere, a mixture of 4 (1 g, 0.95 mmol) and acetyl chloride (20 mL) were added to a 100 mL dried three-neck round-bottom flask. Then the mixture was stirred at 60 °C for 12 h. After the reaction, the solvent was removed at 60 °C under reduced pressure. The residue was washed with hexane and filtered to produce a

black-green solid. The crude product was not purified and used directly for the next step. MALDI-TOF-MS: m/z = 1035.000 (M^+).

Synthesis of compound QIP.

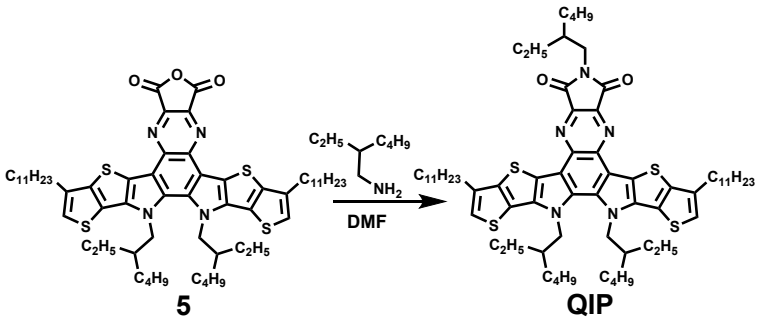

To a 100 mL three-neck round-bottomed flask, a mixture solution of 5 (1 g, 0.97 mmol), 2-ethylhexan-1-amine (0.62 g, 4.83 mmol) and DMF (20 mL) were added under a N_2 atmosphere. Then the mixture was stirred at 100 °C for 12 hours. After cooling to room temperature, the mixture was extracted with dichloromethane, dried with anhydrous Na_2SO_4, filtered and concentrated under reduced pressure. The crude product was further purified by silica gel column chromatography (eluent: petroleum ether/dichloromethane, v/v = 4:1) to yield a yellow solid (0.90 g, 81 %). ^{1}H NMR (400 MHz, $CDCl_3$), δ (ppm): 7.03 (s, 2H), 4.73–4.69 (m, 4H), 3.84–3.82 (d, 2H), 2.76–2.73 (t, 4H), 2.21–2.20 (d, 2H), 2.00–1.98 (t, 1H), 1.83–1.80 (t, 4H), 1.62 (m, 2H), 1.44–1.29 (m, 36H), 1.16–0.87 (m, 30H), 0.69–0.65 (m, 12H); ^{13}C NMR (100 MHz, $CDCl_3$), δ (ppm): 164.75, 143.09, 140.17, 137.09, 136.45, 136.03, 130.80, 124.49, 121.88, 121.37, 118.65, 117.40, 54.20, 41.07, 38.86, 37.64, 30.91, 29.71, 29.29, 28.66, 28.65, 28.57, 28.55, 28.46, 28.35, 27.83, 27.67, 26.67, 22.95, 22.13, 22.08, 22.01, 21.80, 21.68, 13.11, 12.73, 9.45, 9.17. MALDI-TOF-MS: m/z = 1145.887 (M^+).

Synthesis of compound QIP-CHO.

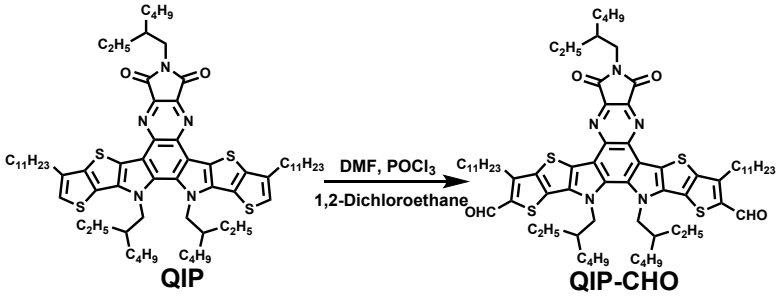

To a solution of compound QIP (0.8 g, 0.70 mmol) in dry 20 mL 1,2-dichloroethane and 5 mL DMF was dropped 0.8 mL of phosphorus oxychloride at 0 °C under the protection of nitrogen. The mixture was stirred at 0 °C for 1 h. After refluxing at 85 °C overnight, the mixture was poured into ice water (100 mL), neutralized with Na_2CO_3 (aq), and then extracted with dichloromethane. The combined organic layer was washed with water and brine, dried over anhydrous Na_2SO_4. After removal of solvent, the crude product was purified by silica gel using petroleum ether/dichloromethane (2:1, v/v) as eluent, yielding an orange solid (0.70 g, 83 %). ^{1}H NMR (400 MHz, $CDCl_3$), δ (ppm): 10.15 (s, 2H), 4.77–4.71 (m, 4H), 3.84–3.83 (d, 2H), 3.15–3.13 (t, 4H), 2.16 (m, 2H), 1.98–1.96 (t, 1H), 1.87–1.84 (t, 4H), 1.63 (m, 4H), 1.43–1.25 (m, 28H), 1.15–0.85 (m, 36H), 0.73–0.65 (m, 12H); ^{13}C NMR (100 MHz, $CDCl_3$), δ (ppm): 181.91, 165.24, 146.90, 144.87, 142.07, 138.06, 137.76, 137.44, 132.85, 132.81, 128.86, 127.03, 118.78, 55.48, 42.33, 40.12, 38.69, 31.90, 30.73, 30.58, 29.73, 29.67, 29.62, 29.57, 29.40, 29.33, 28.67, 28.23, 27.62, 27.57, 24.00, 23.19, 23.02, 22.79, 22.69, 14.12, 13.72, 10.48, 10.29, 10.25. MALDI-TOF-MS: m/z = 1202.745 (M^+).

Synthesis of compound QIP-4F.

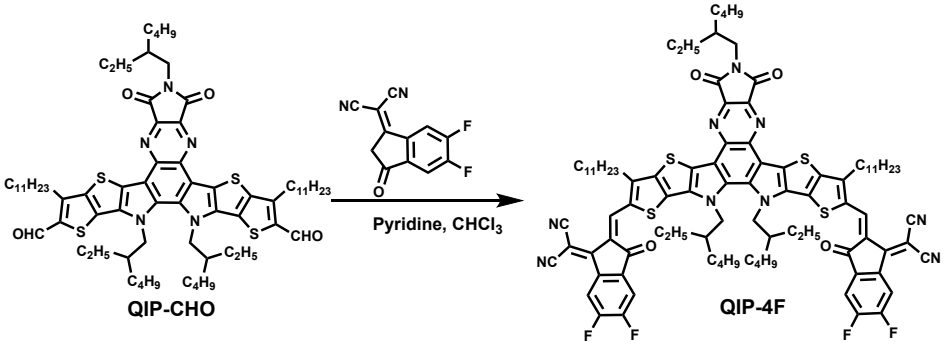

Compound QIP-CHO (0.15 g, 0.12 mmol) and 2-(5,6- difluoro-3-oxo-2,3-dihydro-1H-inden-1-ylidene)malononitrile (0.17 g, 0.72 mmol) were dissolved in chloroform (60 mL). Pyridine (1 mL) was added under argon. After stirring at 65 °C overnight, the mixture was cooled to room temperature, and the solution was concentrated under reduced pressure, and poured into methanol and filtered. The crude product was purified by silica gel using petroleum ether/dichloromethane (2:1, v/v) as eluent, yielding a reddish-dark blue solid (0.16 g, 81 %). ^{1}H NMR (400 MHz, $CDCl_3$), δ (ppm): 9.14 (s, 2H), 8.56–8.52 (m, 2H), 7.76–7.73 (t, 2H), 4.92–4.87 (t, 4H), 3.83–3.81 (d, 2H), 3.16 (t, 4H), 2.30 (m, 2H), 1.94 (m, 1H), 1.92–1.77 (t, 4H), 1.42–1.23 (m, 56H), 0.96–0.82 (m, 20H), 0.76–0.72 (m, 6H); ^{13}C NMR (100 MHz, $CDCl_3$), *δ* (ppm): 186.23, 164.78, 158.50, 155.52, 155.41, 153.92, 153.46, 153.41, 153.35, 153.30, 146.34, 142.32, 138.50, 138.37, 138.36, 136.74, 136.71, 136.67, 135.19, 134.86, 134.57, 134.52, 133.51, 133.22, 130.00, 120.47, 119.58, 115.07, 114.90, 114.77, 114.39, 112.56, 112.42, 69.17, 56.06, 42.33, 40.38, 38.61, 31.95, 31.46, 30.75, 29.97, 29.87, 29.71, 29.66, 29.63, 29.60, 29.52, 29.36, 28.60, 27.79, 24.01, 23.41, 23.34, 23.08, 22.98, 22.69, 14.11, 14.07, 13.89, 13.83, 10.48, 10.42, 10.41. MALDI-TOF-MS: m/z = 1627.014

(M^+).

Synthesis of compound QIP-4Cl.

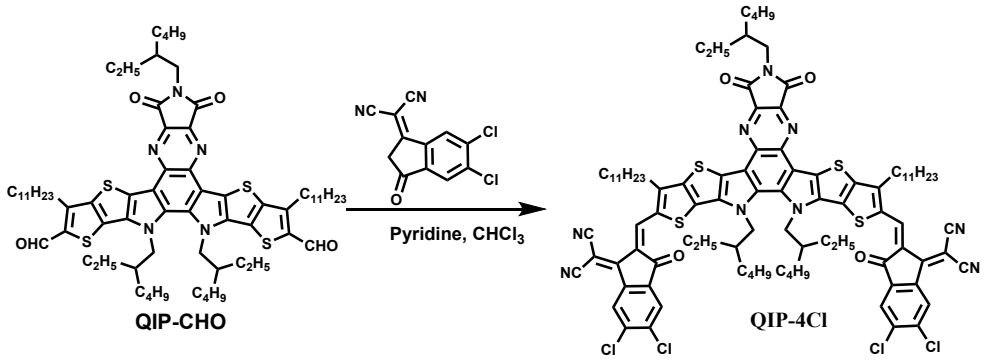

Compound QIP-CHO (0.15 g, 0.12 mmol) and 2-(5,6-dichloro-3-oxo-2,3-dihydro-1H-inden-1-ylidene)malononitrile (0.19 g, 0.72 mmol) were dissolved in chloroform (60 mL). Pyridine (1 mL) was added under argon. After stirring at 65 °C overnight, the mixture was cooled to room temperature, and the solution was concentrated under reduced pressure, and poured into methanol and filtered. The crude product was purified by silica gel using petroleum ether/dichloromethane (2:1, v/v) as eluent, yielding a reddish-dark blue solid (0.17 g, 83 %). ^{1}H NMR (400 MHz, $CDCl_3$), δ (ppm): 9.14 (s, 2H), 8.74 (s, 2H), 8.01 (d, 2H), 4.93–4.89 (t, 4H), 3.83–3.81 (d, 2H), 3.16 (t, 4H), 2.31 (m, 2H), 1.92 (m, 1H), 1.81–1.77 (t, 4H), 1.44–1.23 (m, 56H), 0.89–0.82 (m, 20H), 0.75–0.72 (m, 6H); ^{13}C NMR (100 MHz, $CDCl_3$), δ (ppm): 186.31, 164.82, 158.46, 154.18, 146.60, 142.53, 139.64, 139.29, 138.77, 138.53, 138.44, 136.08, 135.81, 135.29, 133.62, 133.59, 130.46, 126.95, 125.06, 120.43, 119.60, 114.88, 114.41, 69.26, 56.01, 42.39, 40.40, 38.62, 31.94, 31.48, 30.74, 29.97, 29.82, 29.72, 29.68, 29.66, 29.64, 29.60, 29.53, 29.36, 28.60, 27.77, 24.01, 23.40, 23.36, 22.98, 22.70, 14.12, 14.09, 13.84, 10.44, 10.43, 10.41. MALDI-TOF-MS: m/z = 1692.763 (M^+).

2. Instruments and measurements

Nuclear magnetic resonance spectra were collected on a Bruker AVANCE 500 spectrometer using tetramethylsilane (TMS) as the internal standard. MALDI-TOF-MS spectra was measured on a BrukerBIFLEXIII mass spectrometer. UV–vis absorption spectra of the NFAs samples in diluted chloroform solutions (1×10^{-5} M) and in thin films cast onto quartz glass were performed by using a HP 8453 spectrophotometer. Cyclic voltammetry (CV) experiments of NFAs thin films were carried out on an electrochemistry workstation (CHI660e, Chenhua Shanghai) using a conventional three-electrode configuration, including a Pt working electrode, a Pt wire counter electrode, a Hg/Hg_2Cl_2 reference electrode. An anhydrous and N_2 saturated acetonitrile solution containing 0.1 M tetrabutylammonium hexylfluorophosphate (*n*-Bu_4NPF_6) was employed as the electrolyte. The Platinum stick electrode drop-coated with a thin layer of NFAs film was used as the working electrode. The HOMO and LUMO levels were calculated according to the formula $E_{HOMO} = -e[E_{ox} + 4.80 - E(_{Fc/Fc^+})]$ eV and $E_{LUMO} = -e[E_{red} + 4.80 - E(_{Fc/Fc^+})]$ eV, where E_{ox} and E_{red} were determined from the onset oxidation and reduction potentials, respectively, by using ferrocene/ferrocenium (Fc/Fc^+) as the internal standard (0.39 V vs. Hg/Hg_2Cl_2). Differential scanning calorimetry (DSC) were recorded on a DSC214 at a heating rate of 10 °C min^{-1} under a nitrogen flow rate of 20 mL min^{-1}.

The current density-voltage (*J*–*V*) characteristics were measured using a computer-controlled Keithley 2400 SourceMeter under 1 sun irradiation from an AM 1.5 G solar

simulator (Taiwan, Enlitech, SS-F5). Tapping-mode AFM images were obtained by using a Bruker multimode microscope. TEM images were measured using a JEM-2100F. GIWAXS measurements were performed at beamline 7.3.3 of Advanced Light Source, Lawrence Berkeley National Laboratory. The x-ray beam energy was 10 keV. The sample to detector distance was ~276 mm calibrated with Silver Behenate and the incidence angle was 0.16^{o} normalized by a photodiode. The scattering signals were imaged in Helium atmosphere using a 2D charge-coupled device (CCD) detector (Pilatus 2M) with a pixel size of 0.172 mm × 0.172 mm. The film samples were spincoated on PEDOT:PSS/silicon wafer substrates, and further treatments were consistent with device fabrications.

3. Fabrication of PSCs

All of the solar cell devices with a conventional configuration of ITO/PEDOT:PSS/active layer/PFN-Br/Ag were fabricated. Firstly, the ITO glass substrates were pre-cleaned sequentially by using detergent, ethanol, acetone, and isopropyl alcohol under sonication, and dried in oven at 75 °C for 6 h before to use. Followed by treating with oxygen plasma for 1 min, the PEDOT:PSS was spin-coated onto the ITO glass at 3000 rpm for 30 s and then annealed at 150 °C for 20 min in air. Subsequently, the substrates were transferred into a N_2-protected glove box for spin-coating the active layer. The donor polymer P2F-EHp and the small molecule acceptors, QIP-4F or QIP-4Cl, were dissolved in CF solution (with variant blend ratios, the total concentration of the donor polymer and the acceptor is 5.5 mg mL^{-1}). The mixed solution was spin-coated atop the PEDOT:PSS layer at 1000 rpm for 20 s in CF containing 0.5 vol% DBE to form the active layer with a film thicknesses approximately 100 nm. Then, the active layers were treated with thermal annealing at 110 °C for 10 min. Finally, the interface layer (5 nm) of PFN-Br in methanol (0.5 mg mL^{-1}) was spin-coated on the blended films, and then the top electrode silver (100 nm) was deposited onto the interlayer PFN-Br by thermal evaporation though a shadow mask in a vacuum chamber with a base pressure of 1×10^{-6} mbar. The active layer area of the device was 0.04 cm^2.

Fabrication and Characterization of Charge-only Devices

The hole-only and electron-only mobilities of P2F-EHp: acceptors blend films and

the acceptor neat films were determined from space-charge-limited current (SCLC) devices. The hole mobility was measured in a hole-only device with the configuration of ITO/PEDOT:PSS/active layer/Ag. The electron mobility was measured in an electron-only device with the configuration of ITO/ZnO/active layer/PFNDI-Br/Ag. The ZnO sol-gel was obtained from stirring the solution of 1.0 g $Zn(CH_3COO)_2 \cdot 2H_2O$ in 10 mL ethylene glycol monomethyl ether and 275 μL ethylenediamine at 60 °C for 12 h. The total concentration of P2F-EHp and the small molecule acceptors, QIP-4F or QIP-4Cl, was fixed at 5.5 $mg \cdot mL^{-1}$, and the blend films were obtained by spin-coating the P2F-EHp: acceptor (1 : 1, w/w) blend solution in CF containing 0.5 vol% DBE to obtain active layer of with a film thicknesses approximately 100 nm. The mobilities were determined by fitting the dark *J*–*V* current to the model of a single carrier SCLC which were calculated on the basis of the following equation:

$$J = (9/8)\, \varepsilon_0 \varepsilon_r \mu V_{eff}^2 / d^3$$

where J is the current density, μ is the charge (hole or electron) mobility at zero field, ε_0 is the permittivity of free space, ε_r is the relative permittivity of the material, d is the thickness of the active layer, and V_{eff} is the effective voltage ($V - V_{bi}$). The charge (hole or electron) mobility was calculated from the y intercept of the *J*–*V* curves.

4. Supporting Figures

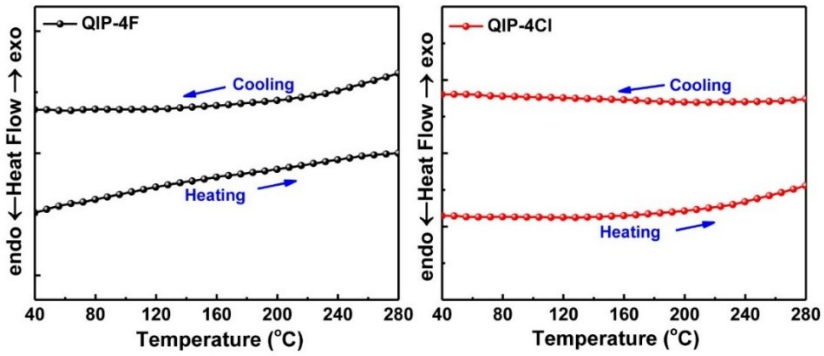

Fig. S1 DSC curve of QIP-4F and QIP-4Cl measured under N_2 atmosphere.

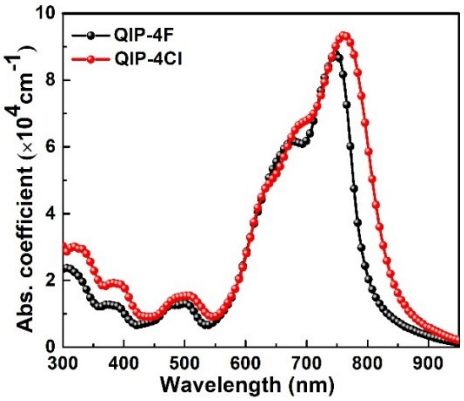

Fig. S2 Molar extinction coefficient of QIP-4F and QIP-4Cl in film state.

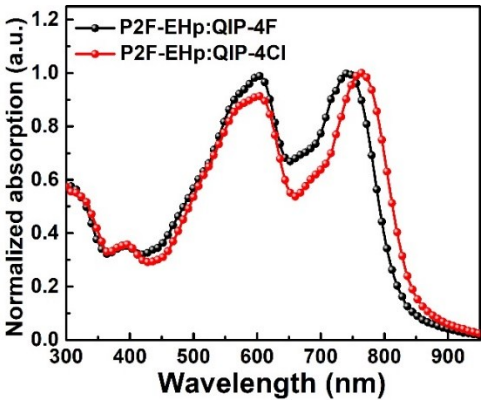

Fig. S3 Normalized UV–vis absorption spectra of P2F-EHp:QIP-4F and P2F-EHp:QIP-4Cl in blend films.

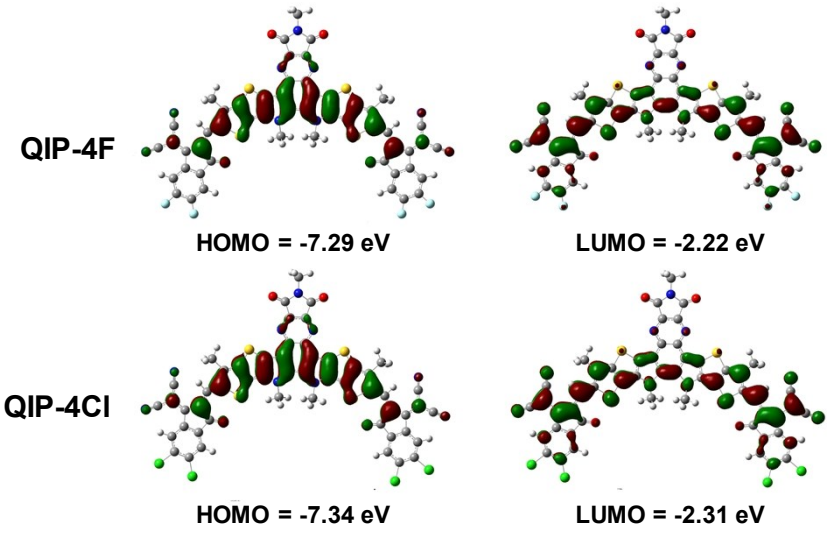

Fig. S4 HOMO and LUMO orbital distributions and energy levels calculated by DFT/□B97X-D/6-31+G (d,p), the alkyl side chains on the central core (QIP) were replaced by $-CH_3$ groups to simplify the calculations.

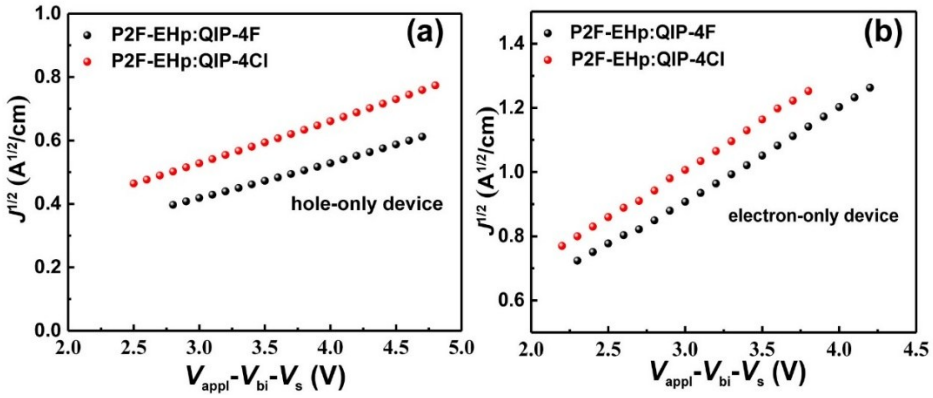

Fig. S5 (a) SCLC hole mobility for P2F-EHp:QIP-4F and P2F-EHp:QIP-4Cl films; (b) SCLC electron mobility for P2F-EHp:QIP-4F and P2F-EHp:QIP-4Cl films.

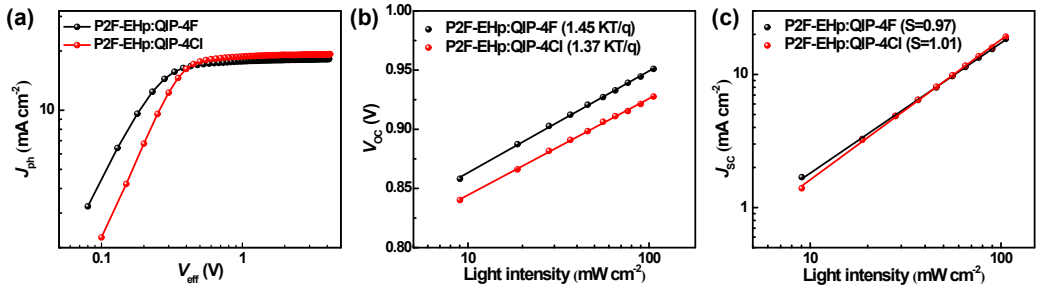

Fig. S6 (a) J_{ph} versus V_{eff} characteristics, (b) V_{oc} versus light intensity, (c) J_{sc} versus light intensity (P_{light}) characteristics for PSCs based on P2F-EHp:QIP-4F and P2F-EHp:QIP-4Cl.

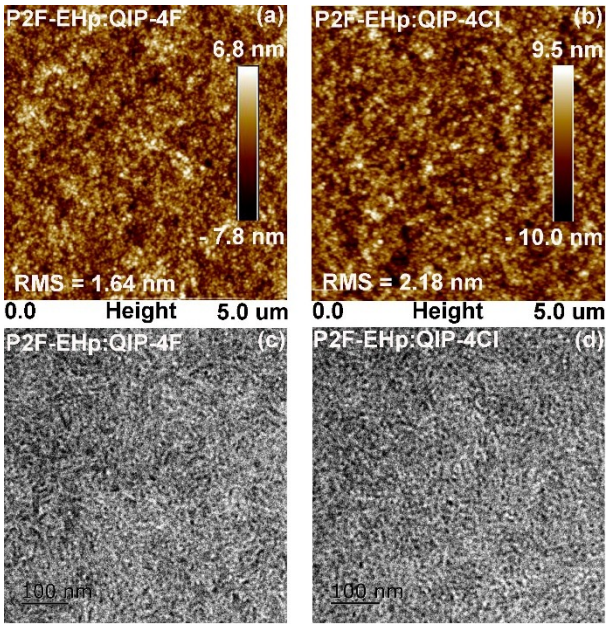

Fig. S7 AFM height images (5 × 5 μm) of P2F-EHp:QIP-4F (a) and P2F-EHp:QIP-4Cl (b) blend films with 0.5% DBE additive; TEM images of P2F-EHp:QIP-4F (c) and P2F-EHp:QIP-4Cl (d) blend films with 0.5% DBE additive.

5. Supporting Tables

Table S1 Photophysical and electrochemical properties of QIP-4F and QIP-4Cl in solution and in thin films.

acceptor	λ_s, max [a] [nm]	λ_f, max [b] [nm]	λ_{onset} [nm]	E_g^{opt} [c] [eV]	HOMO [eV]	LUMO [eV]	E_g^{CV} [eV]
QIP-4F	700	750	806	1.54	– 5.75	– 3.86	1.89
QIP-4Cl	718	762	839	1.48	– 5.77	– 3.89	1.88

[a] The maximum absorption in solution. [b] The maximum absorption in film. [c] $E_g = 1240/\lambda_{onset}$.

Table S2 The summaries of the photophysical properties of the quinoxalineimide (QI), benzo[2,1,3]thiadiazole (BTz) and benzoquinoxaline (BQ)-based fused-ring small-molecule acceptors reported to date in the related literatures.

acceptor	λ_f, max [a] [nm]	E_g^{opt} [b] [eV]	HOMO [eV]	LUMO [eV]	ε_f,max (cm^{-1})	Ref.
Y6	821	1.33	– 5.65	– 4.10	1.07×10^5	1
BTP-Cl	839	N/A	– 5.68	– 4.12	1.09×10^5	3
AQx-1	N/A [c]	1.35	– 5.59	– 3.85	N/A	4
AQx-2	830	1.35	– 5.62	– 3.88	N/A	5
QIP-4F	750	1.54	– 5.75	– 3.86	8.8×10^4	This work
QIP-4Cl	762	1.48	– 5.77	– 3.89	9.4×10^4	This work

[a] The maximum absorption in film. [b] $E_g = 1240/\lambda_{onset}$. [c] N/A : not available.

Table S3. Photovoltaic properties of the PSCs based on P2F-EHp as donor and QIP-4F or QIP-4Cl as the acceptor with different solvent additive ratios under AM 1.5 G at 100 mW cm^{-2}.

Donor:Acceptor (w/w)	DBE (%)	V_{oc} (V)	J_{sc} (mA cm^{-2})	FF (%)	PCE (%)
P2F-EHp:QIP-4F (1:1)	0	1.02	15.02	40.40	6.19
	0.3	0.93	18.24	71.08	12.09
	0.5	0.94	18.27	70.53	12.11
	1	0.93	17.34	72.87	11.75
	1.5	0.93	15.70	74.19	10.83
P2F-EHp:QIP-4Cl (1:1)	0	1.00	14.78	42.25	6.24
	0.3	0.94	19.51	71.35	13.09
	0.5	0.94	19.62	72.11	13.30
	1	0.92	18.87	73.12	12.69
	1.5	0.92	17.07	72.56	11.39

Table S4. Photovoltaic properties of the PSCs based on P2F-EHp as donor and QIP-4F or QIP-4Cl as the acceptor with different thermal annealing (TA) temperatures under AM 1.5 G at 100 mW cm^{-2}.

Donor:Acceptor (w/w)	TA (°C)	V_{oc} (V)	J_{sc} (mA cm^{-2})	FF (%)	PCE (%)
P2F-EHp:QIP-4F (1:1)	100	0.93	17.81	72.33	12.04
	110	0.94	18.27	70.53	12.11
	120	0.93	17.33	73.18	11.82
P2F-EHp:QIP-4Cl (1:1)	100	0.93	19.63	71.16	13.03
	110	0.94	19.62	72.11	13.30
	120	0.93	19.58	70.42	12.86

Table S5. Photovoltaic properties of the PSCs based on P2F-EHp as donor and QIP-4F or QIP-4Cl as the acceptor with different active layer thickness under AM 1.5 G at 100 mW cm^{-2}.

Donor:Acceptor (w/w)	Thickness (nm)	V_{oc} (V)	J_{sc} (mA cm^{-2})	FF (%)	PCE (%)
P2F-EHp:QIP-4F (1:1)	95	0.95	17.46	70.04	11.62
	100	0.94	18.27	70.53	12.12
	110	0.95	17.16	69.93	11.40
P2F-EHp:QIP-4Cl (1:1)	90	0.93	19.01	72.23	12.77
	100	0.94	19.62	72.11	13.30
	110	0.92	19.42	69.26	12.37

Table S6. Summary of quinoxalineimide-based devices for OSCs in the literature.

Entries	Acceptor	Donor	V_{oc} (V)	J_{sc} (mA cm^{-2})	FF (%)	PCE (%)	Ref.
1	QI-Th	P3HT	0.80	0.84	39	0.33	3
2	QI-BiTh	P3HT	0.85	0.91	35	0.34	3
3	QIP-4F	P2F-EHp	0.94	18.27	70.53	12.11	This work
4	QIP-4Cl	P2F-EHp	0.94	19.62	72.11	13.30	This work

Table S7. The summaries of the photovoltaic properties of the quinoxalineimide (QI), benzo[2,1,3]thiadiazole (BTz) and benzoquinoxaline (BQ)-based fused-ring small-molecule acceptors based binary OSCs reported to date in the related literatures.

Entries	Acceptor	Donor	V_{oc} (V)	J_{sc} (mA cm^{-2})	FF (%)	PCE (%)	Ref.
1	Y6	PM6	0.83	25.3	74.8	15.7	1
2	BTP-Cl	PBDB-TF	0.867	25.4	75.0	16.5	4
3	AQx-1	PBDB-TF	0.89	22.18	67.14	13.31	5
4	AQx-2	PBDB-TF	0.86	25.38	76.25	16.64	5
5	QIP-4F	P2F-EHp	0.94	18.27	70.53	12.11	This work
6	QIP-4Cl	P2F-EHp	0.94	19.62	72.11	13.30	This work

Table S8. SCLC electron (hole) mobility measurements for P2F-EHp:QIP-4F and P2F-EHp:QIP-4Cl films.

Active layer [a]	μ_h (cm^2 V^{-1} s^{-1})	μ_e (cm^2 V^{-1} s^{-1})	Thickness (nm)
P2F-EHp:QIP-4F	0.74×10^{-4}	4.71×10^{-4}	~100
P2F-EHp:QIP-4Cl	1.04×10^{-4}	5.32×10^{-4}	~100

[a] All of the blend films were processed by CF containing 0.5 vol% DBE and treated with 110 ^{o}C for 10 min.

Table S9. Relevant parameters obtained from J_{ph}–V_{eff} curves.

Active layer [a]	$J_{SC,\ EQE}$ [b] (mA cm^{-2})	J_{ph} [c] (mA cm^{-2})	J_{sat} (mA cm^{-2})	$P(E,T)$[c] (%)	L (nm)
P2F-EHp:QIP-4F	18.04	18.53	18.99	97.58	~100
P2F-EHp:QIP-4Cl	19.37	19.65	19.85	98.98	~100

[a] All of the blend films were treated with 110 ^{o}C for 10 min ; ; [b] Obtained from the integration of EQE spectra. [c] At the condition of $V_{eff} = V_0 - V_{appl}$ (V_{appl} = 0, under short-circuit condition)

6. NMR Spectra

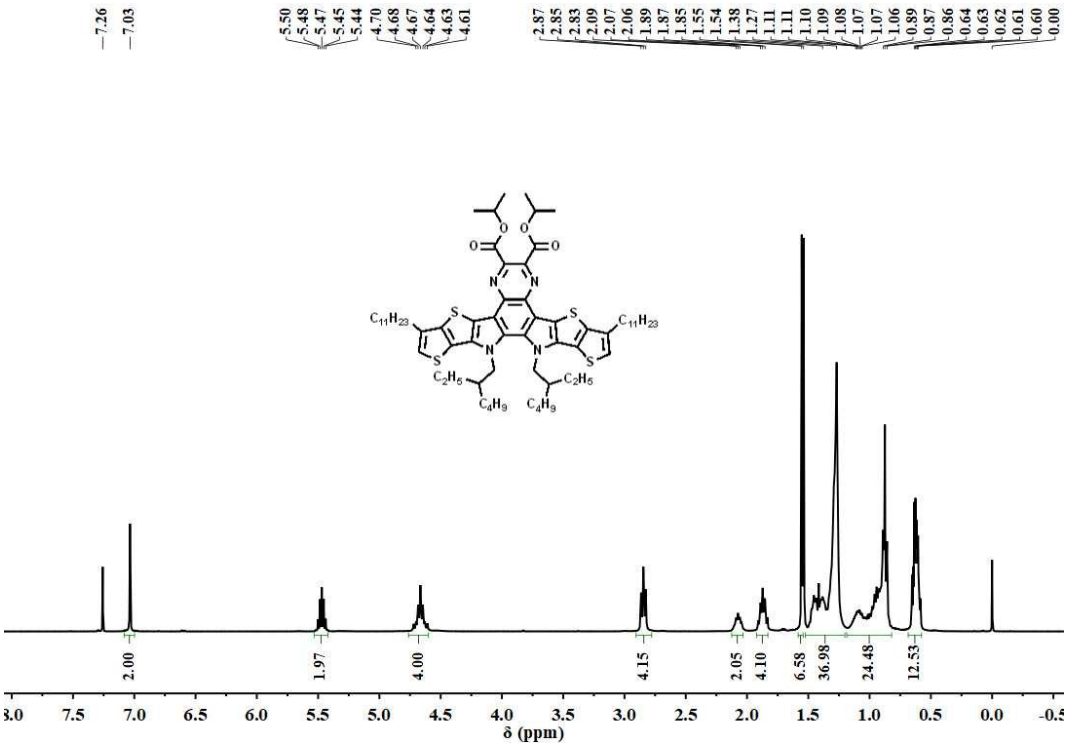

Fig. S8 ^{1}H NMR spectrum of compound 3 in $CDCl_3$

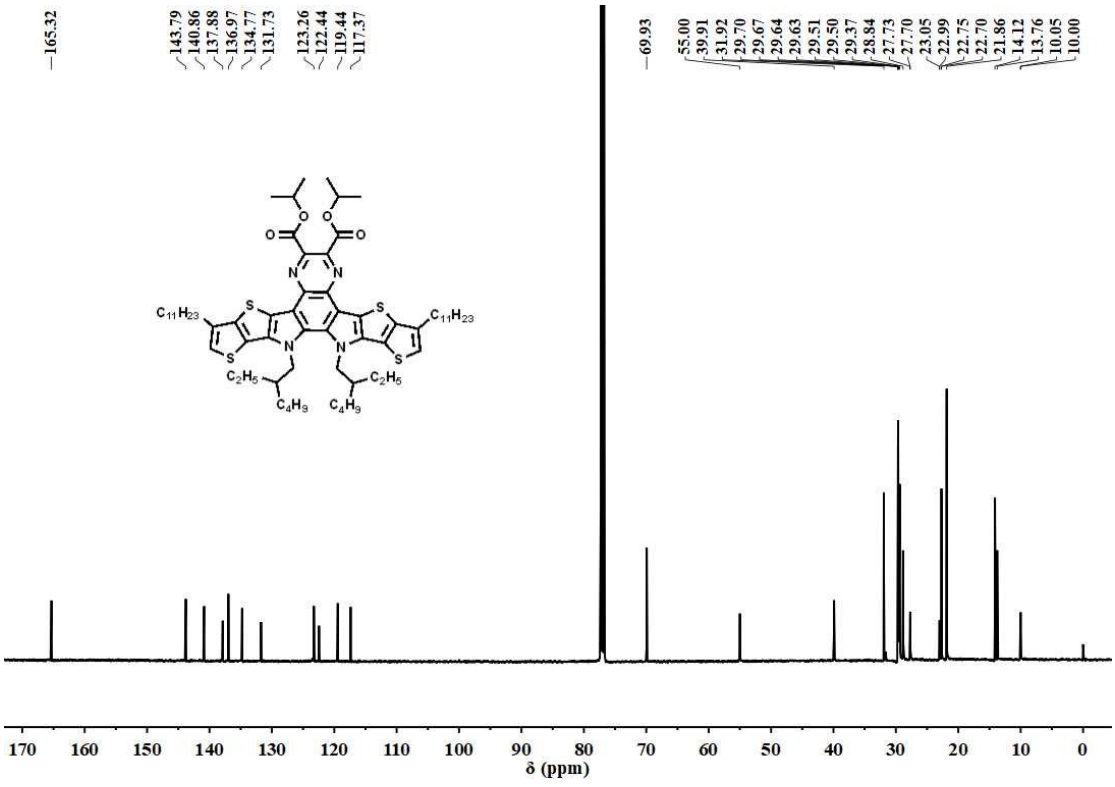

Fig. S9 ^{13}C NMR spectrum of compound 3 in $CDCl_3$

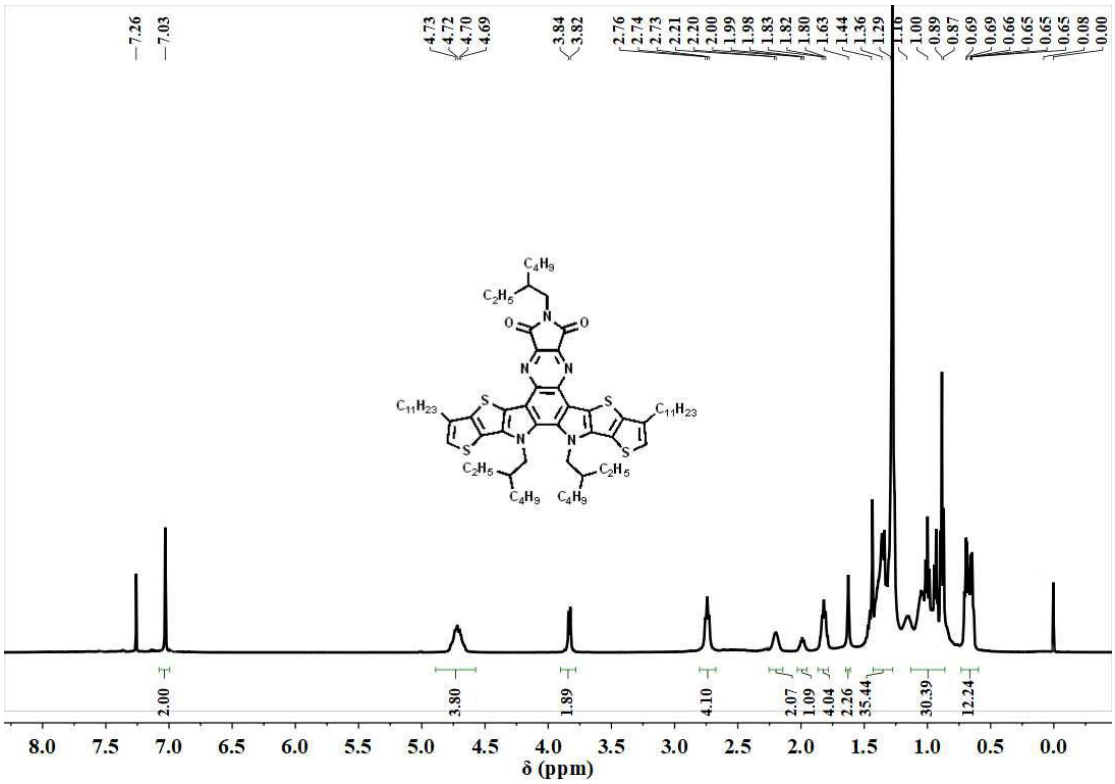

Fig. S10 ^{1}H NMR spectrum of compound QIP in $CDCl_3$

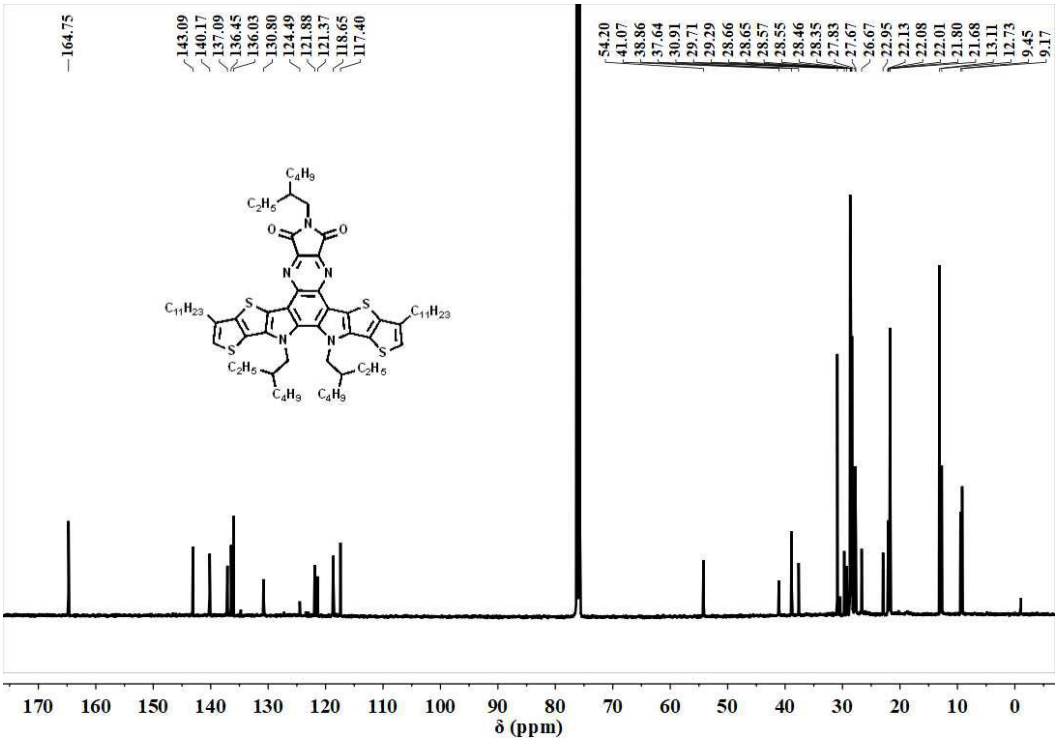

Fig. S11 ^{13}C NMR spectrum of compound QIP in $CDCl_3$

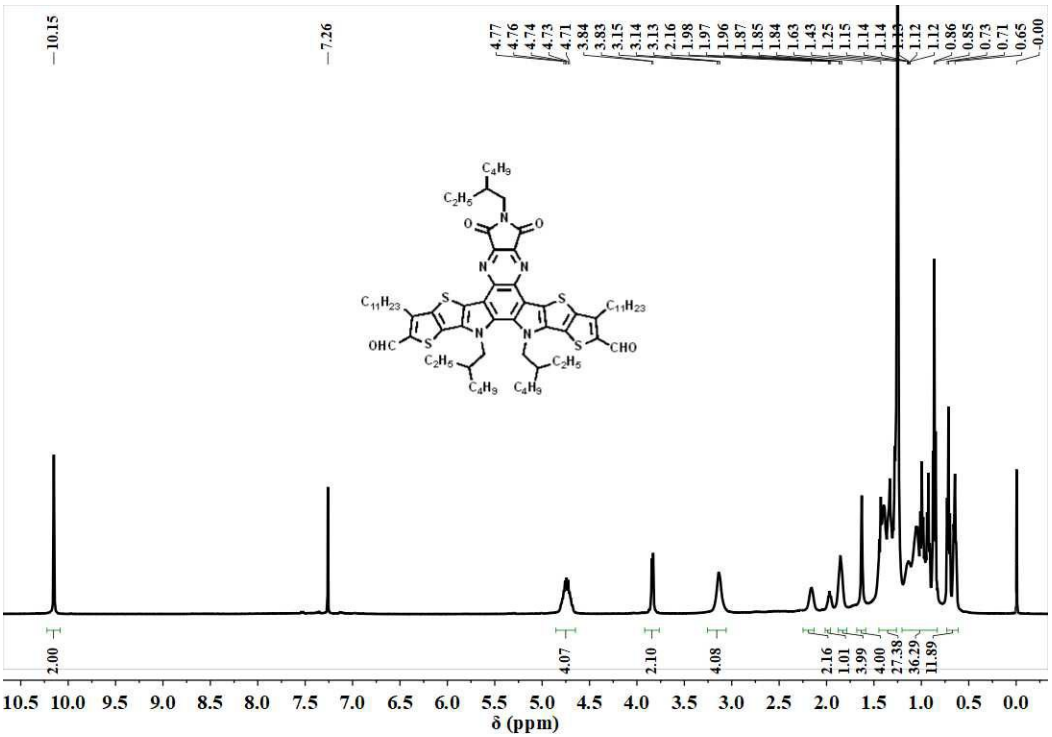

Fig. S12 ^{1}H NMR spectrum of compound QIP-CHO in $CDCl_3$

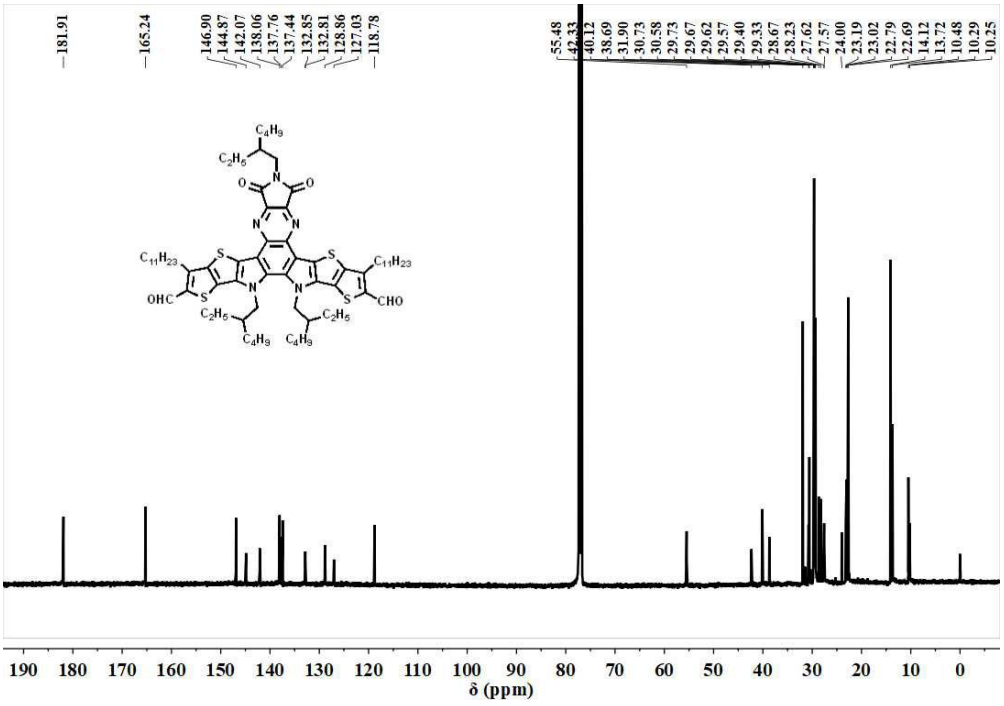

Fig. S13 ^{13}C NMR spectrum of compound QIP-CHO in $CDCl_3$

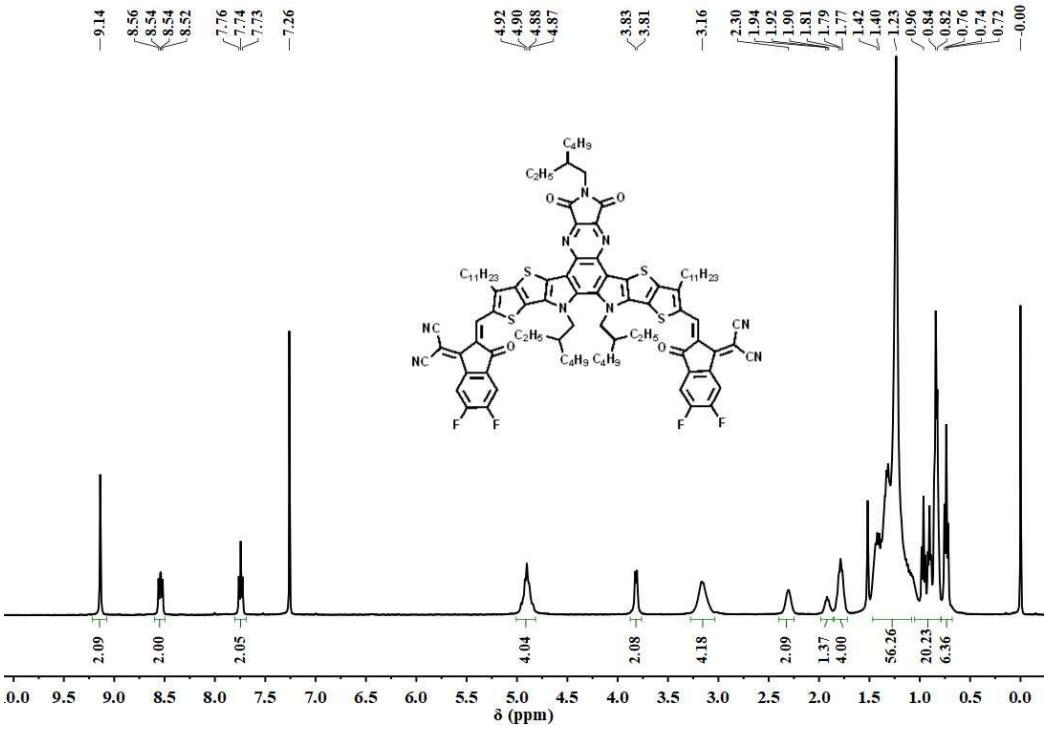

Fig. S14 ^{1}H NMR spectrum of compound QIP-4F in $CDCl_3$

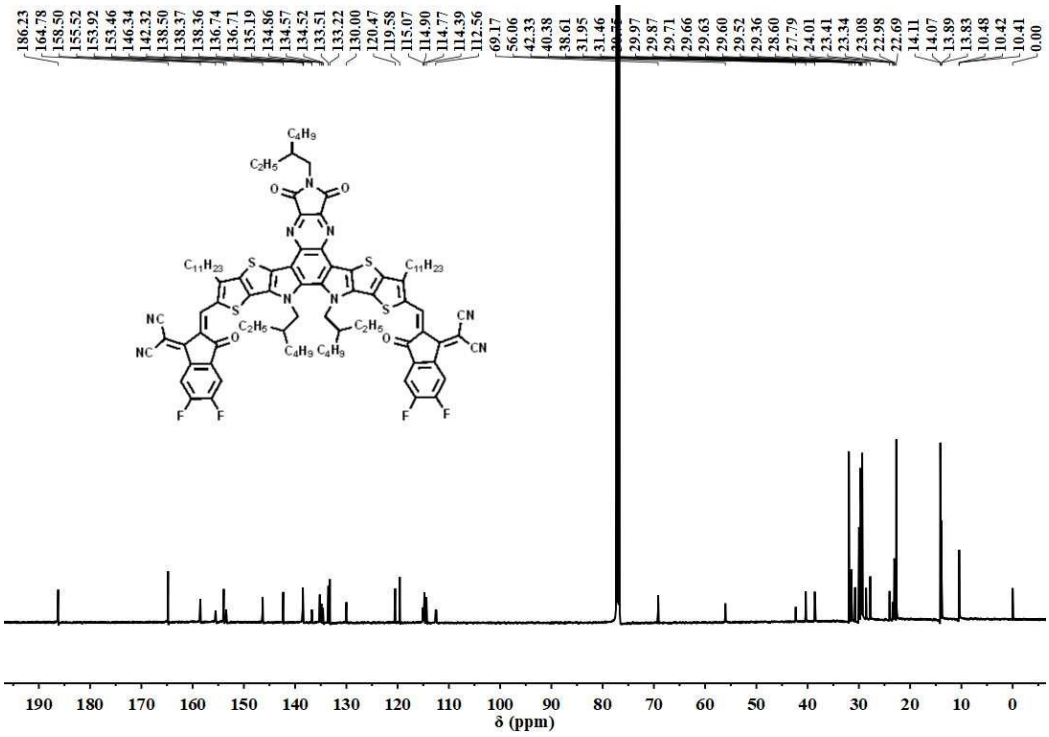

Fig. S15 ^{13}C NMR spectrum of compound QIP-4F in $CDCl_3$

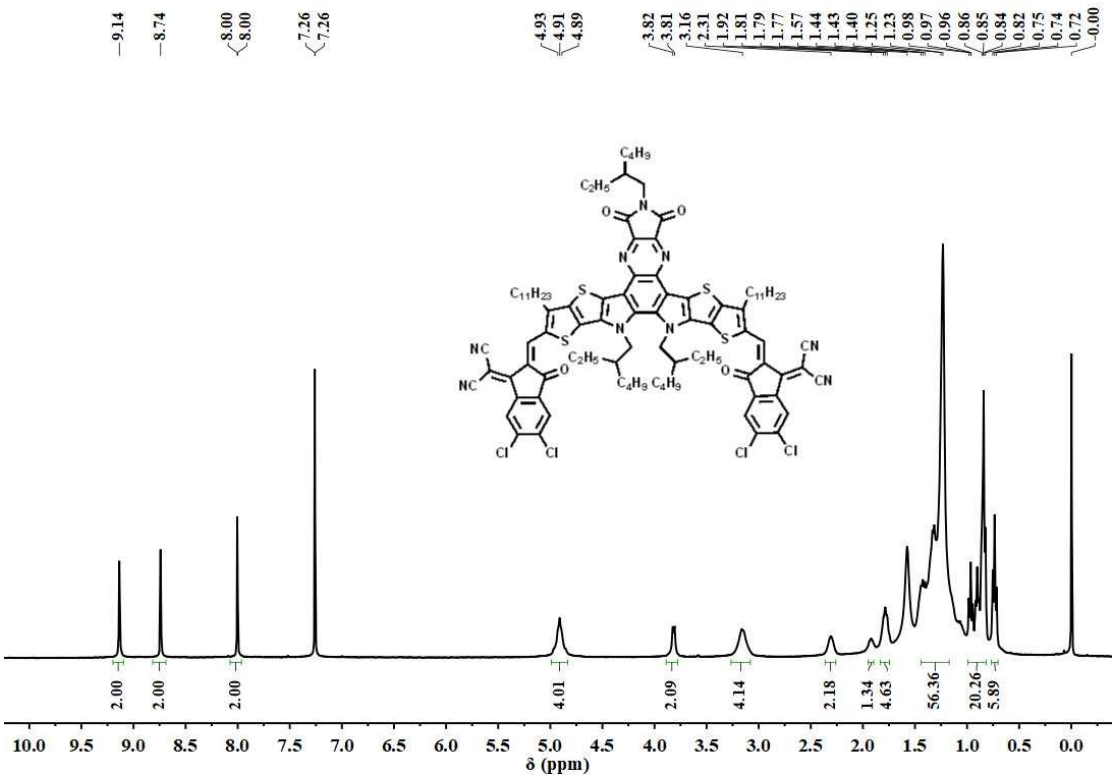

Fig. S16 ^{1}H NMR spectrum of compound QIP-4Cl in $CDCl_3$

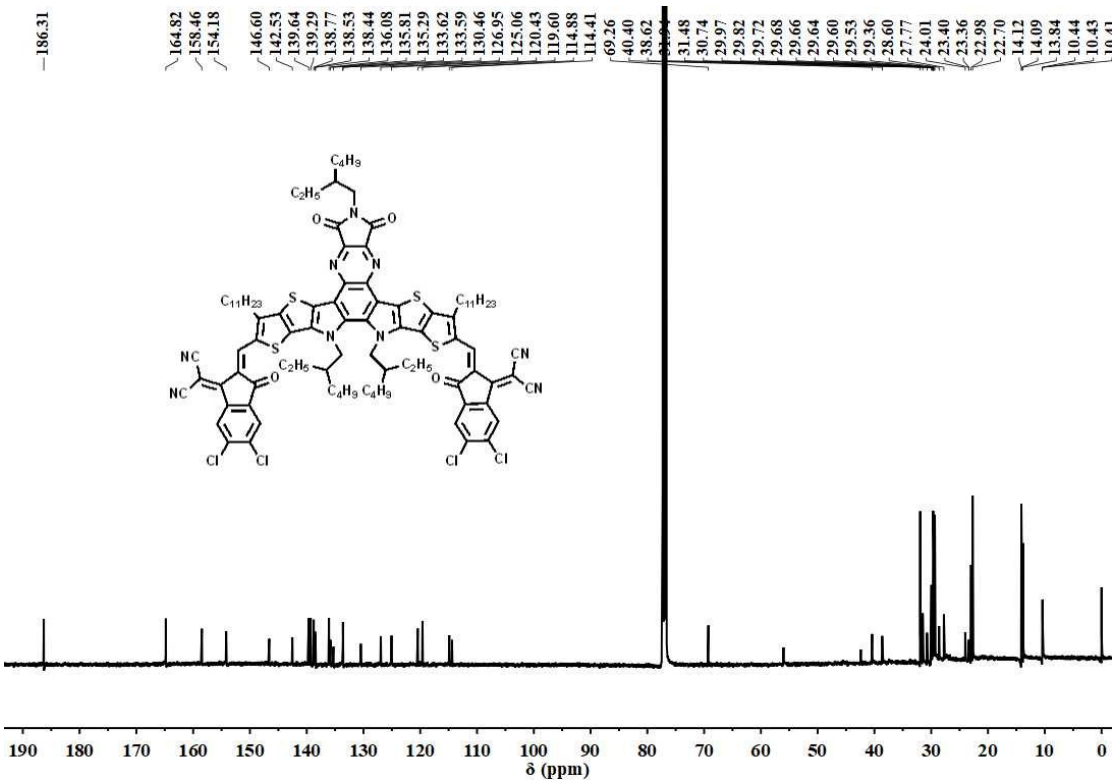

Fig. S17 ^{13}C NMR spectrum of compound QIP-4Cl in $CDCl_3$

7. References

1 J. Yuan, Y. Zhang, L. Zhou, G. Zhang, H.-L. Yip, T.-K. Lau, X. Lu, C. Zhu, H. Peng, P. A. Johnson, M. Leclerc, Y. Cao, J. Ulanski, Y. Li and Y. Zou, *Joule*, 2019, **3**, 1140.

2 T. Hasegawa, K. Aoyagi, M. Ashizawa, Y. Konosu, S. Kawauchi, N. S. Sariciftci, and H. Matsumoto, *Chem. Lett.*, 2015, **44**, 1128.

3 Y. Cui, H. Yao, J. Zhang, T. Zhang, Y. Wang, L. Hong, K. Xian, B. Xu, S. Zhang, J. Peng, Z. Wei, F. Gao and J. Hou, *Nat. Commun*., 2019, **10**, 2515.

4 Z. Zhou, W. Liu, G. Zhou, M. Zhang, D. Qian, J. Zhang, S. Chen, S. Xu, C. Yang, F. Gao, H. Zhu, F. Liu and X. Zhu, *Adv. Mater.*, 2020, **32**, 1906324.